

Interplay between perturbative and non-perturbative effects in the stealthy Higgs model

R. Akhouri¹, J.J. van der Bij^{1,2}, H. Wang¹

¹ The Randall Laboratory of Physics, University of Michigan, Ann Arbor, MI 48109-1120, USA

² Fakultät für Physik, Universität Freiburg, H.-Herder-Str. 3, 79104 Freiburg, Germany

Received: 24 October 2000 /

Published online: 8 June 2001 – © Springer-Verlag / Società Italiana di Fisica 2001

Abstract. We study corrections to electroweak precision variables in a model with strongly interacting singlet Higgs particles.

1 Introduction

With the close of the LEP experiments the structure of the weak interactions as a gauge theory has been fully confirmed. The only missing ingredient at the moment is direct evidence of the Higgs sector. The LEP-200 experiment gives a lower bound of $m_H > 113$ GeV [1]. The precision measurements at LEP-1 and SLC imply a relatively low Higgs mass (< 170 GeV) [2], though some lingering doubts remain because of the different values for the hadronic and leptonic data.

If the Higgs boson is indeed light and of the standard model type, it should be easy to find at the LHC. However, the precision data do not prove that this is indeed the case. There are still two possibilities for the Higgs boson to remain hidden at the LHC. The first is that the Higgs boson is simply too heavy to be produced. Within the standard model this implies strong interactions. In that case the limit on the Higgs boson mass, which comes from one-loop calculations, is not reliable. While the two-loop corrections are small and cannot provide for a fit to a heavy Higgs boson, the full higher order results could be different. There are some indications in the literature that resumming bubble graphs in the Higgs propagator can lead to a saturation of the radiative corrections. The second way to hide a Higgs boson at the LHC is by the introduction of singlet Higgs fields [3–11]. In this case there are two effects. One is mixing of the doublet and singlet Higgs boson, leading to a split of the Higgs peak into different peaks, each being less significant than a single standard model peak. The second effect is the possibility of decay into invisible singlet particles. The invisible decay width is not necessarily small, so one could have a light Higgs particle with a large invisible width. One can also combine mixing and invisible decay, to generate a Higgs signal spread out over an arbitrary energy range with a large invisible decay fraction. Such a Higgs signal would be extremely hard to identify at the LHC, since there is no

peak in the signal compared to the background. The signal would be an overall enhancement of the missing energy. For this to be useful, one has to know the background very precisely. The background cannot be calculated precisely at the LHC; however, at a high energy e^+e^- collider there is no problem in looking for this signal. It is important to point out here that an additional phenomenological advantage of introducing the singlet Higgs fields is that they would be prime candidates for self-interacting cold dark matter. In fact, the model introduced in the next section is the simplest one with WIMPs.

There is therefore a realistic possibility that the LHC will not see evidence for the Higgs sector. That means that the only information would consist of the LEP precision measurements. It is for this reason, that we decided to look more carefully at the radiative corrections in the invisible Higgs scenario. As both a large width and strong interactions can play a role we decided to study the radiative corrections in the so-called stealthy Higgs model [9].

We describe the model in Sect. 2. In Sect. 3 we discuss some analytical results for the simplest case, to gain some understanding on the difference between the all order bubble resummation from the $1/N$ expansion and the results of finite order in perturbation theory. In Sect. 4 we give numerical results.

2 The Higgs $O(N)$ singlet model

To illustrate the consequences of a hidden sector coupled to the Higgs boson in a possibly strong way, we want to consider the case of scalar gauge singlets – let us call them “phions” – added to the SM. To deal with the case of strong interactions we introduce an N -plet of such phions. This allows us to use non-perturbative $1/N$ methods. Neglecting all the fermions and gauge couplings for the moment, our model consists of the SM Higgs sector coupled

to an $O(N)$ symmetric scalar model. Similar models can be found in [5–7]. Our Lagrangian density is

$$L_{\text{scalar}} = L_{\text{Higgs}} + L_{\text{phion}} + L_{\text{interaction}},$$

where

$$\begin{aligned} L_{\text{Higgs}} &= -\partial_\mu \phi^\dagger \partial^\mu \phi - \lambda \left(\phi^\dagger \phi - \frac{v^2}{2} \right)^2, \\ L_{\text{phion}} &= -\frac{1}{2} \partial_\mu \varphi \partial^\mu \varphi - \frac{1}{2} m_P^2 \varphi^2 - \frac{\kappa}{8N} (\varphi^2)^2, \\ L_{\text{interaction}} &= -\frac{\omega}{2\sqrt{N}} \varphi^2 \phi^\dagger \phi. \end{aligned} \quad (1)$$

Here we use a metric with signature $(-+++)$. $\phi = (\sigma + v + i\pi_1, \pi_2 + i\pi_3)/2^{1/2}$ is the complex Higgs doublet of the SM with the vacuum expectation value $\langle 0|\phi|0\rangle = (v/2^{1/2}, 0)$, $v = 246$ GeV. Here, σ is the physical Higgs boson and $\pi_{i=1,2,3}$ are the three Goldstone bosons. $\varphi = (\varphi_1, \dots, \varphi_N)$ is a real vector with $\langle 0|\varphi|0\rangle = \mathbf{0}$. If we would allow for a non-vanishing vacuum expectation value for the phions, the mass matrix would become non-diagonal and Higgs–phion mixings would occur. The lightest scalar of the gauged model would have a reduced coupling to the vector bosons by the cosine of a mixing angle. We will not discuss this possibility further, as we are mainly interested in the effects coming from the Higgs width. If we look at the gauged model we can choose the unitary gauge to rotate away the unphysical Goldstone bosons. This is gauge invariant, because in the following we only consider loops of gauge singlet particles. Note that the vacuum induced mass term for the phions is suppressed by a factor $1/N^{1/2}$.

In the case of large non-standard couplings ω and κ , loop induced operators with external Higgs and phion fields appear and are not negligible. They are only suppressed by powers of $1/N$. For the discussion of Higgs signatures, it is enough to focus on the Higgs propagator.

As shown above the propagator is modified by the phions. In the leading order in $1/N$, which is found in the limit $N \rightarrow \infty$, the Higgs self-energy is given by an infinite sum of phion bubble terms. Regularization of the divergent bubbles, i.e. absorbing the divergent and some constant contributions into the bare parameters, is done by subtraction of the logarithmically divergent part. With this regularization, the Euclidean bubble integral

$$\begin{aligned} I_{\text{bubble}}(s = -p^2, m_\phi^2) &= \frac{1}{2} \int \frac{d^4 k}{(2\pi)^4} \frac{1}{k^2 + m_\phi^2} \frac{1}{(k+p)^2 + m_\phi^2} \end{aligned}$$

becomes above the phion threshold

$$\begin{aligned} I(s, \mu^2, m_\phi^2) &= I_{\text{bubble}}(s, m_\phi^2) - I_{\text{bubble}}(0, \mu^2) \\ &= -\frac{1}{32\pi^2} \left(\log \left(\frac{m_\phi^2}{\mu^2} \right) - 2 + \sqrt{1 - \frac{4m_\phi^2}{s}} \right) \end{aligned}$$

$$\times \left(\log \left(\frac{1 + \sqrt{1 - \frac{4m_\phi^2}{s}}}{1 - \sqrt{1 - \frac{4m_\phi^2}{s}}} \right) - i\pi \right), \quad (2)$$

with the arbitrary renormalization scale μ . In the case of massless phions this simply reduces to $I(s, \mu^2, 0) = -1/(32\pi^2)(\log(s/(e\mu)^2) - i\pi)$. The bubble sum is the geometric series of the integral times a coupling.

Adding all regularized terms gives the inverse Higgs propagator

$$\begin{aligned} D_H^{-1}(s, \mu^2) &= -s + M_H^2 - i\sqrt{s}\Gamma_{SM}(s) + \Sigma(s, \mu^2), \\ \Sigma(s, \mu^2) &= \frac{-\omega^2 v^2 I(s, \mu^2, m_\phi^2)}{1 + \kappa I(s, \mu^2, m_\phi^2)}. \end{aligned} \quad (3)$$

Above the phion threshold, $s > 4m_\phi^2$, Σ develops an imaginary part which results in a Higgs width depending on the non-standard parameters leading to observable effects. The independent SM Higgs width is added, too. To find an explicit expression for the upper propagator, remember that within the SM the Higgs mass, or better the quartic Higgs coupling, is a free parameter.

Defining the mass by the location of the resonance on the real p^2 -axis fixes our renormalization scale μ by the equation

$$\text{Re}(\Sigma(M_H^2, \mu^2)) = 0. \quad (4)$$

Using this relation, the abbreviations $\tilde{\omega}^2 = \omega^2/(32\pi^2)$, $\tilde{\kappa} = \kappa/(32\pi^2)$ and $r(x) = (1 - 4m_\phi^2/x)^{1/2}$, one finds, after splitting the integral in its real and imaginary part,

$$\begin{aligned} I(s, \mu^2, m_\phi^2)|_{\mu \text{ fixed}} &= a(s) + ib(s), \\ a(s) &= \left(\sqrt{1 - (2\pi\tilde{\kappa}r(M_H^2))^2} - 1 \right) / (2\tilde{\kappa}) \\ &\quad + r(M_H^2) \log \left(\frac{1 + r(M_H^2)}{1 - r(M_H^2)} \right) - r(s) \log \left(\frac{1 + r(s)}{1 - r(s)} \right), \\ b(s) &= \pi r(s), \end{aligned}$$

an expression for the Higgs propagator, in terms of running quantities:

$$\begin{aligned} D_H^{-1}(s) &= -s + M_H(s)^2 - i\sqrt{s}\Gamma_H(s), \\ M_H(s)^2 &= M_H^2 - \tilde{\omega}^2 v^2 \frac{a(s) + \tilde{\kappa}(a(s)^2 + b(s)^2)}{(1 + \tilde{\kappa}a(s))^2 + (\tilde{\kappa}b(s))^2}, \\ \Gamma_H(s) &= \Gamma_{SM}(s) + \frac{\tilde{\omega}^2 v^2}{\sqrt{s}} \frac{b(s)}{(1 + \tilde{\kappa}a(s))^2 + (\tilde{\kappa}b(s))^2}. \end{aligned} \quad (5)$$

Remember that this expression is only valid above the phion threshold.

The advantage of this model is that one can study separately the effect of a strong coupling ω of the standard model Higgs to the hidden sector and of strong interactions κ within the hidden sector. Thereby one separates the effects of a large width from the effects of strong interactions. We mention that the standard model in the $1/N$ expansion [12–15] is reproduced within this model by taking $m_H^2 = 2\lambda v^2$ and $\omega = \kappa = 2\lambda$.

3 Analytical considerations

In this chapter we discuss some analytical results. At first sight this would appear to be a hopeless undertaking, because of the complicated form of the propagator. Also there seems to be no reason to do so. Naively one would take simply the non-perturbative Higgs propagator, insert it in the diagrams and calculate the result numerically. This has indeed been tried in the literature [13–15]. However, this procedure has a problem due to the presence of a tachyon in the propagator and one will not get finite results. In order to better understand what is going on, it is therefore advantageous to attempt an analytic calculation. This is clearly not possible in the general case. We will study therefore the simplified case $m_P = 0$ and $\kappa = 0$. Physically we have an unstable Higgs particle with a width determined by the coupling ω . The Higgs propagator simplifies to

$$D_H^{-1} = -s + m_H^2 + \Gamma \log(-s/m_H^2 - i\epsilon),$$

with $\Gamma = (\omega^2 v^2)/(32\pi^2)$. We limit the discussion in this chapter to the so-called ρ parameter, which is the ratio of neutral to charged current strengths. We have

$$\rho = G_F^0/G_F^+.$$

At the tree level $\rho = 1$; the correction is given by

$$\delta\rho = \rho - 1 = (\delta M_W^2 - \cos^2(\theta_W)\delta M_Z^2)/M_W^2,$$

where δM_W^2 and δM_Z^2 are the corrections to the vector boson masses at $k^2 = 0$. The ρ parameter is one of the parameters measured in the electroweak tests. It is related to the commonly used T parameter by $T = (1 - \rho^{-1})/\alpha$.

3.1 The standard model

Within the standard model the one-loop Higgs mass dependent correction to $\delta\rho$ is simplest described in the unitary gauge. Here only one diagram contributes, the tadpole-like graphs containing the $2H-2W$ vertex cancel in $\delta\rho$. One finds, using dimensional regularization, with n the dimension of spacetime,

$$\begin{aligned} \delta\rho &= \frac{-g^2}{(2\pi)^{4i}} \left(1 - \frac{1}{n}\right) \\ &\times \left(\int d^n k (k^2 + M_W^2)^{-1} (k^2 + m_H^2)^{-1} \right. \\ &\left. - \frac{1}{\cos^2(\theta_W)} \int d^n k (k^2 + M_Z^2)^{-1} (k^2 + m_H^2)^{-1} \right). \end{aligned}$$

The contribution from these Higgs dependent graphs is still infinite, of the form

$$\delta\rho = -\frac{3g^2}{64\pi^2} \text{tg}^2(\theta_W) (2/(n-4) + \log(m_H^2) + \text{finite}). \quad (6)$$

The infinite piece cancels against the infinities coming from the pure W boson graphs, that are independent of

the form of the Higgs propagator. The explicit form of the finite part is quite complicated. To get a simple result for the Higgs mass dependence only, we subtract the contribution for the fictitious case $m_H = 0$:

$$\begin{aligned} &\delta\rho(\text{SM}; m_H) - \delta\rho(\text{SM}; m_H = 0) \\ &= -\frac{3g^2}{64\pi^2} \left(\frac{1}{\cos^2(\theta_W)} \frac{m_H^2}{m_H^2 - M_Z^2} \log(m_H^2/M_Z^2) \right. \\ &\quad \left. - \frac{m_H^2}{m_H^2 - M_W^2} \log(m_H^2/M_W^2) \right). \end{aligned}$$

In the limit $\text{tg}(\theta_W) \rightarrow 0$ this simplifies to

$$\begin{aligned} &\delta\rho(\text{SM}; m_H) - \delta\rho(\text{SM}; m_H = 0) \\ &= -\frac{3g^2}{64\pi^2} \text{tg}^2(\theta_W) \left(\frac{m_H^2}{m_H^2 - M_W^2} \log(m_H^2/M_W^2) \right), \end{aligned}$$

showing the close connection between the ρ parameter and the hypercharge coupling. If we further assume that $m_H \gg M_W$ one can simply express the ρ parameter by the integral

$$\delta\rho = \frac{g^2}{(2\pi)^{4i}} \text{tg}^2(\theta_W) \left(1 - \frac{1}{n}\right) \int d^n k (k^2)^{-1} (k^2 + m_H^2)^{-1}.$$

This form is useful for the more elaborate calculations later on. In the large Higgs mass limit one finds therefore

$$\begin{aligned} &\delta\rho(\text{SM}; m_H) - \delta\rho(\text{SM}; m_H = 0) \\ &= -\frac{3g^2}{64\pi^2} \text{tg}^2(\theta_W) \log(m_H^2/M_W^2). \quad (7) \end{aligned}$$

3.2 Two-loop result

The correction $\delta\rho_2$ at the two-loop level can be straightforwardly calculated using the techniques of [16,17]. Experience from the standard model where it was found that $\delta\rho_2 \approx m_H^2$ would lead one to expect that in our model $\delta\rho_2 \approx \omega^2 v^2/m_H^2$. However an explicit calculation gives

$$\begin{aligned} \delta\rho_2 &= \frac{3g^2\omega^2 v^2}{4096\pi^4} \left(\frac{M_W^2}{(m_H^2 - M_W^2)^2} \log^2(m_H^2/M_W^2) \right. \\ &\quad \left. - \frac{1}{\cos^2(\theta_W)} \frac{M_Z^2}{(m_H^2 - M_Z^2)^2} \log^2(m_H^2/M_Z^2) \right). \end{aligned}$$

This shows that for large Higgs mass the two-loop correction is suppressed compared to naive expectations. This might be a clue as to why the standard model coefficient of the two-loop corrections to electroweak quantities is very small. Indeed the inclusion of the two-loop heavy Higgs corrections within the standard model do not significantly affect the electroweak fits. This might therefore indicate that the first large corrections would appear at the three-loop level in the ρ parameter. Indeed it is known from calculations in the standard model, that only at the two-loop level there are large changes in the Higgs propagator. Since the ρ parameter probes the Higgs propagator indirectly, two-loop corrections in the Higgs propagator translate into three-loop corrections in the ρ parameter. In any case the above result shows that it is important to check what happens at higher order.

3.3 All orders perturbation theory

To calculate the all orders results we work in the limit where the Higgs mass is large and $\text{tg}(\theta_W)$ small, so that we can ignore the mass of the vector bosons within the diagrams. Going to Euclidean space a diagram with n -phion bubbles can then be written in the form

$$\int d^4k \frac{1}{k^2} \frac{1}{(k^2 + m_H^2)^{n+1}} \log^n(k^2/m_H^2).$$

Going to polar coordinates the $1/k^2$ factor cancels in the d^4k integration, thereby simplifying the integrals. Keeping the coupling constants we find

$$\delta\rho = \frac{3g^2 \text{tg}^2(\theta_W)}{64\pi^2} \sum_{n=1}^{\infty} \int_0^{\infty} (-\Delta)^n \frac{\log^n(s)}{(s+1)^{n+1}} ds,$$

where

$$\Delta = \frac{\omega^2 v^2}{32\pi^2 m_H^2}.$$

The integrals can be performed explicitly, giving

$$\delta\rho = \frac{3g^2 \text{tg}^2(\theta_W)}{64\pi^2} \sum_{n=2}^{\infty} \frac{(-2\pi\Delta)^n}{n} |B_n| (1 - 2^{1-n}),$$

where B_n are the Bernoulli numbers. Since the odd Bernoulli numbers are 0, only the graphs with an even number of phion bubbles contribute, which explains the suppression found in the previous section. The series found above is clearly divergent. The question is whether it is resumable. The Borel sum is defined as follows. Given the above series $\sum_{n=2}^{\infty} a_n \Delta^n$ we form the new ‘‘Borel’’ series $F(z) = \sum_{n=2}^{\infty} a_n z^{n-1}/(n-1)!$. We find

$$F(z) = \frac{\pi}{\sin(\pi z)} - \frac{1}{z}.$$

The Borel transform has an infinity of poles for positive values of the coupling constant Δ . This means that there is no unambiguous way to resum the perturbative series, so that non-perturbative effects must be present. We will return to the significance of this result for vacuum instability in the next section.

3.4 Non-perturbative contribution

Given the fact that the perturbation theory does not converge, we try to calculate the correction to $\delta\rho$ by first resumming the phion bubbles within the propagator and then inserting the dressed propagator in the diagram. The most efficient way to calculate $\delta\rho$ is to use the Kallén–Lehmann representation for the Higgs propagator:

$$D_H(k^2) = \int ds' \sigma(s') / (k^2 + s' - i\epsilon).$$

Figuratively speaking we thereby write the Higgs propagator as the sum (integral) of a number of Higgses with different masses. The contribution to $\delta\rho$ is then a weighted sum over the different Higgs masses:

$$\delta\rho = \int ds' \sigma(s') \delta\rho(m_H^2 = s'), \quad (8)$$

where $\delta\rho(m_H^2 = s')$ is given in (7). For the propagator to be physical it is necessary that the spectral weight $\sigma(s')$ is positive and is unequal to zero, only for $s' > 0$. The latter is not the case; the resummed propagator contains at least a tachyon. Suppose that the location of a tachyon pole is given by $m_T^2 = -s_0 m_H^2$, with s_0 the solution of the equation $s_0 + 1 + \Delta \log(s_0) = 0$. The residue at the pole is given by $-s_0/(\Delta + s_0)$. Let us assume for the moment that there is only a single tachyon pole. The pole structure of the propagator is examined in detail in the appendix for different values of the parameters. There it is found that depending on the parameters there can be in general more than one unphysical pole, however for the case at hand, i.e., $\tilde{\kappa} = 0$ and massless phions, there is indeed only one tachyonic pole. The simplest way to treat this tachyon pole is to subtract it from the propagator. In that case one finds an at first sight acceptable spectral density:

$$\sigma(s') = \frac{\pi\Gamma}{|-s + m_H^2 + \Gamma \log(s/m_H^2) - i\pi\Gamma|^2}. \quad (9)$$

When one tries to calculate the ρ parameter with this spectral density one runs into a problem. The contribution to $\delta\rho$ coming from a single Higgs boson graph contains a divergence $1/(n-4)$, that gets canceled by the pure vector boson graphs. For the generalized propagator this translates into a contribution $1/(n-4) \int \sigma(s') ds'$. So in order to get a finite contribution to $\delta\rho$ one needs to fulfill the condition $\int \sigma(s') ds' = 1$. This condition is automatically fulfilled at each order in perturbation theory, because of the renormalizability of the theory. The condition is however not fulfilled for the tachyon-subtracted resummed propagator. By a simple contour integral one sees that the difference is indeed due to the tachyon pole:

$$\int ds' \sigma(s') = \Delta/(\Delta + s_0). \quad (10)$$

A graph of the factor as a function of Δ is given in Fig. 1. The effect is non-perturbative as $s_0 \approx \exp(-1/\Delta)$ for $\Delta \rightarrow 0$. Also for very large width the effect becomes small as then $s_0 \rightarrow 1$. The effect is numerically largest for $\Delta = 1$. The presence of the tachyon can be understood as an artefact of the approximation we made. We took into account only the bubble graphs connecting a Higgs boson with two phions. This means that we are effectively dealing with a ϕ^3 theory, thereby having no lowest energy state. The presence of the non-perturbative tachyon thus signifies the possibility of the vacuum being unstable. This vacuum instability was already indicated in the previous subsection by the singularities of the Borel transform on the positive real axis. It is similar to the instability of the QED vacuum against formation of electron–positron pairs in the

presence of strong electric fields [18]. Indeed such considerations already exist in the literature [19]. Using these results and deforming the relevant contours it is easy to determine the imaginary part of the vacuum to vacuum phase (δ) which is related to the probability of vacuum decay. We find

$$\text{Im}\delta = \frac{-i\pi}{e^{1/\Delta} + 1}.$$

This expression exhibits the same qualitative behavior as outlined above.

In the full theory, the spectral density does not just contain the two-phion cut; there are also two-Higgs and multi-phion cuts. Since the full theory has a vacuum the tachyon pole should disappear when all graphs are taken into account. However, finding the exact propagator would mean solving the theory completely. This is not possible at present. As long as we are limited to summing partial sets of graphs such instabilities are bound to be present. To still get a reasonable idea of the possible effects of a large Higgs width, we have to find a phenomenological prescription to deal with this problem. The prescription has to satisfy two conditions: first it should reproduce perturbation theory, second it should satisfy the Källén–Lehmann representation for the Higgs propagator. We chose therefore to do the following. We start with the resummed propagator and subtract the tachyon pole. The resulting spectral density is positive definite and non-zero only for $s' > 0$. It is however not correctly normalized, so we multiply the spectral density with the non-perturbative correction factor $(\Delta + s_0)/\Delta$. This way we keep the shape of the spectral density the same, basically assuming that the spectral density is dominated by the two-phion states. This is not a perfect procedure of course, but lacking the means to solve the theory exactly, it appears the best one can do. From the numbers in Fig. 1 we expect the result not to be too far from the truth.

4 Numerical results

The above considerations are applied in this section to the calculation of $\delta\rho$ and of the S parameter in the stealthy Higgs model.

From the discussion in Sects. 2,3 we may write down the following formulae for these parameters. Consider first the difference of the ρ parameter in the stealthy Higgs model and in the standard model:

$$\begin{aligned} & \delta\rho(\text{sth}, m_H) - \delta\rho(\text{SM}, m_H) \\ &= \frac{3g^2}{64\pi^2} \int_0^\infty ds \bar{\sigma}(s) \left(f(s, M^2) - \frac{1}{c^2} f(s, M_z^2) \right. \\ & \quad \left. - f(m_H, M^2) + \frac{1}{c^2} f(m_H, M_z^2) \right), \end{aligned} \quad (11)$$

$$f(s, M^2) = \frac{s}{s - M^2} \ln \left(\frac{s}{M^2} \right). \quad (12)$$

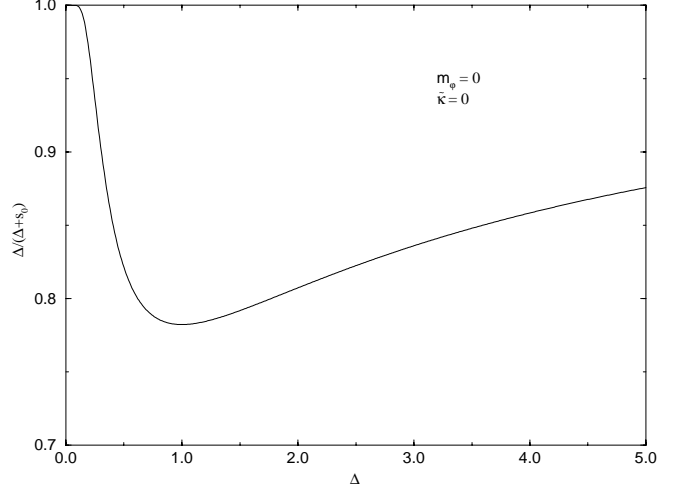


Fig. 1. Non-perturbative propagator correction factor

For the case of massless phions and with $\kappa = 0$, the density $\bar{\sigma}$ is

$$\bar{\sigma}(s) = \frac{\Gamma + s_0 m_H^2}{\left(-s + m_H^2 + \Gamma \ln \frac{s}{m_H^2} \right)^2 + \pi^2 \Gamma^2}. \quad (13)$$

The more general cases are discussed in the appendix. There can be more than one unphysical pole and a subtraction has to be made for all of them. The renormalization factor was determined numerically using the expression for the spectral density that is obtained after subtracting the tachyon pole and checked against the expression (30) in the appendix.

Customarily, the S parameter is defined by

$$\frac{\alpha}{4c^2 s^2} S = \frac{\Pi_{ZZ}(M_Z^2) - \Pi_{ZZ}(0)}{M_Z^2}. \quad (14)$$

From this it is straightforward to obtain the following formula for the difference of this parameter in the stealthy Higgs model and in the SM:

$$\begin{aligned} & S(\text{sth}, m_H) - S(\text{SM}, m_H) \\ &= \frac{-1}{\pi} \int \bar{\sigma}(s) ds (H(s) - H(m_H^2)), \end{aligned} \quad (15)$$

$$\begin{aligned} H(m_H^2) &= \left(\frac{m_H^2}{M_Z^2} \right)^2 \left(-1/12 - 1/12 F(m_H) - \frac{1}{12} \ln \frac{M_Z^2}{m_H^2} \right) \\ & \quad + \frac{m_H^2}{m_H^2 - M_Z^2} \left(-3/4 \ln \frac{M_Z^2}{m_H^2} \right) \\ & \quad + \frac{m_H^2}{M_Z^2} \left(7/24 + 1/3 F(m_H) + 1/4 \ln \frac{M_Z^2}{m_H^2} \right) \\ & \quad - 2 - F(m_H), \end{aligned} \quad (16)$$

$$F(m_H) = \int_0^1 \ln \left(x^2 + \frac{m_H^2}{M_Z^2} (1-x) \right). \quad (17)$$

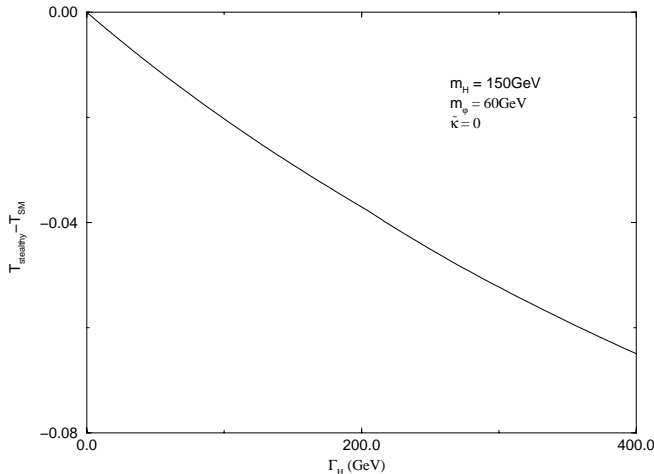


Fig. 2. Correction to the T parameter in the stealth model without self-interactions among the phions

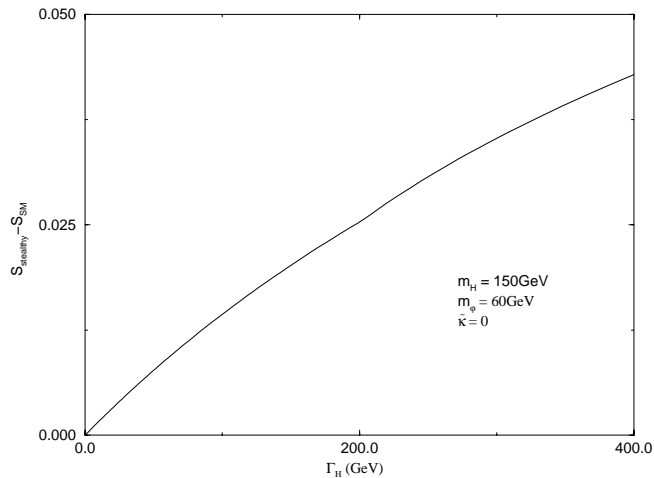


Fig. 3. Correction to the S parameter in the stealth model without self-interactions among the phions

These formulae can now be used to study the radiative corrections for physically interesting cases. As a first example we take $m_H = 150$ GeV, $m_\phi = 60$ GeV, $\kappa = 0$. These parameters are of interest, since they correspond to a typical case, where no evidence would have been seen at LEP, where the LHC is insensitive, but where a linear e^+e^- collider would discover the Higgs boson. With respect to the radiative corrections there are two questions to be discussed here. The first is whether there are significant differences between the stealth model and the standard model. We see from Figs. 2 and 3 that the difference is actually quite small, of the order of a few 10^{-2} , which is within the errors of the measurements. The corrections behave as if one had a somewhat heavier Higgs as in the standard model. If a large width Γ_H gives a contribution, precisely mimicking a heavier Higgs, there is of course still no way to determine whether the precision measurements prefer the standard model or the stealth model. Therefore it is useful to consider the Higgs mass (large Higgs mass) independent contribution $6\pi S + 8/3\pi \cos^2(\theta_W)T$ and see if

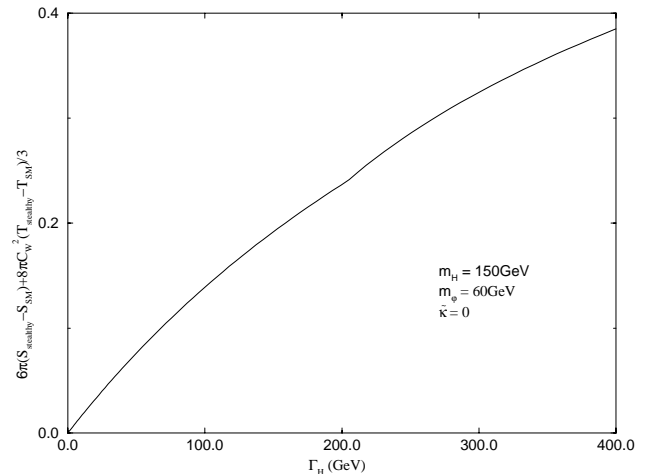


Fig. 4. Correction to a (large) Higgs mass independent quantity in the stealth model without self-interactions among the phions

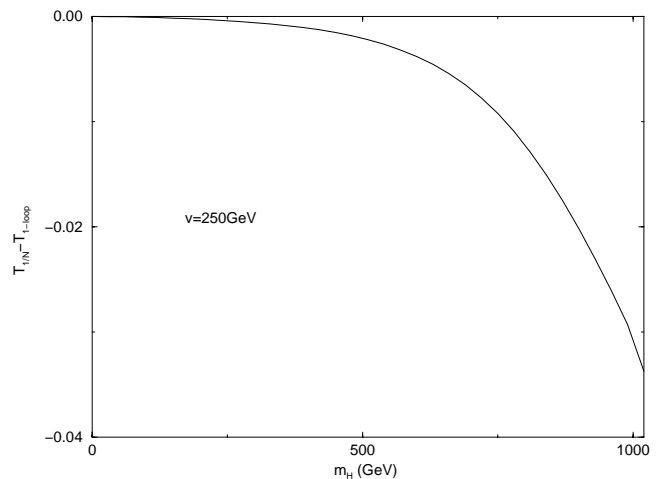


Fig. 5. Correction to the T parameter in the standard model, $1/N$ expansion minus one-loop correction

deviations are present. This combination is given in Fig. 4. We see that a difference is present; however, it is quite small. This example shows, that the precision tests cannot rule out the stealth model as the differences between it and the standard model are small. However the stealth model appears to always mimic a Higgs heavier than the standard model Higgs, for the same value of the mass parameter. Therefore the stealth model cannot generate corrections that would behave as if the Higgs were very light, which appears to be preferred by the leptonic data.

Another case of special interest is the standard model in the $1/N$ limit, which has also been discussed in [12–15]. This model corresponds to $m_H^2 = 2\lambda v^2$, $\omega = \kappa = 2\lambda$. The graphs for the radiative corrections are given in Figs. 5 and 6. It is to be noted here that in the analysis of the $1/N$ limit, we are keeping the vector boson mass fixed. Thus in the figures for this case, we have used $v/N^{1/2}$ for the vacuum expectation value. We see that for a large range of the Higgs mass, up to about 1 TeV there is es-

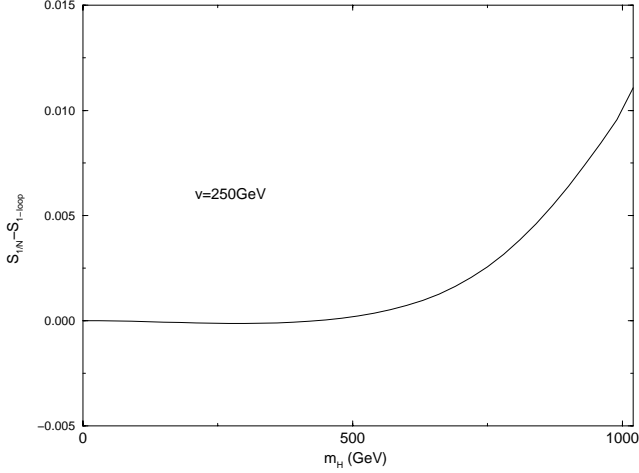


Fig. 6. Correction to the S parameter in the standard model, $1/N$ expansion minus one-loop correction

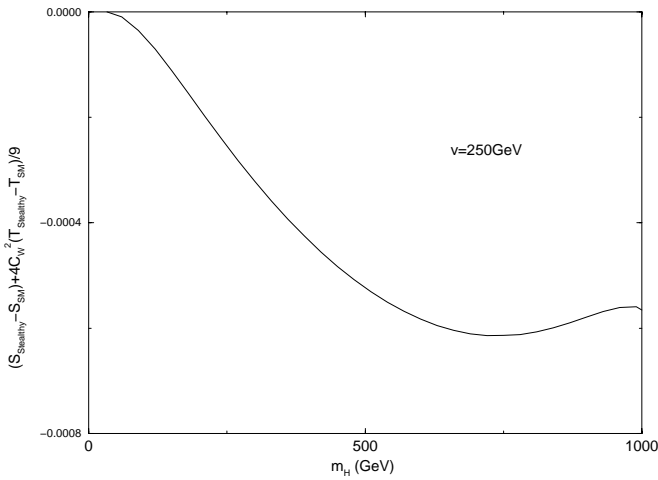


Fig. 7. Correction to a one-loop (large) Higgs mass independent quantity in the standard mode, $1/N$ expansion minus one-loop correction

essentially no change compared to the standard model one-loop corrections. After this scale the strong interactions take over and have the effect, both in S and T , of increasing the large Higgs mass growth of the radiative corrections. This does not happen with S and T in the same way, so that there is a Higgs mass dependence in the sum $6\pi S + 8/3\pi \cos^2(\theta_W)T$ as seen in Fig. 7. This appears to be contrary to the statements in the literature, where a saturation of the radiative corrections is found. There are two important points worth mentioning here. First, we restrict ourselves in this analysis to values of approximately $m_H \leq 1$ TeV. This because of the way we have set up the formalism in Sect. 2 – this constraint is the only way to satisfy (4). It is therefore possible that the saturation sets in at larger values of the Higgs mass. This possibility will be studied in a separate publication. Secondly, it is not clear how previous authors have treated problems with the tachyon. Based on Fig. 7, we therefore conclude that after resummation of the bubble graphs, the large Higgs

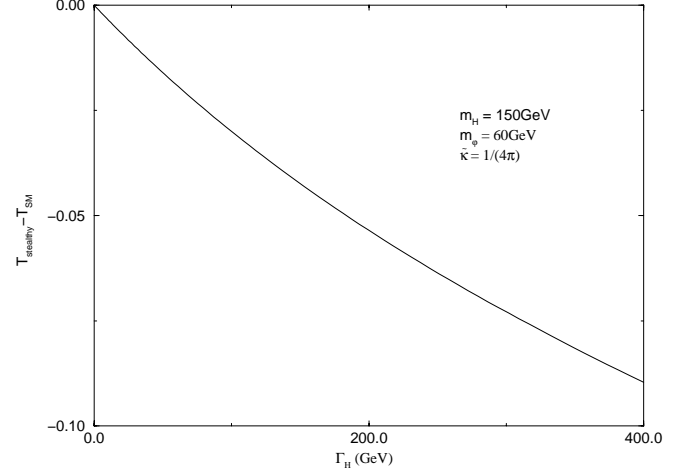


Fig. 8. Correction to the T parameter in the stealth model with self-interactions among the phions

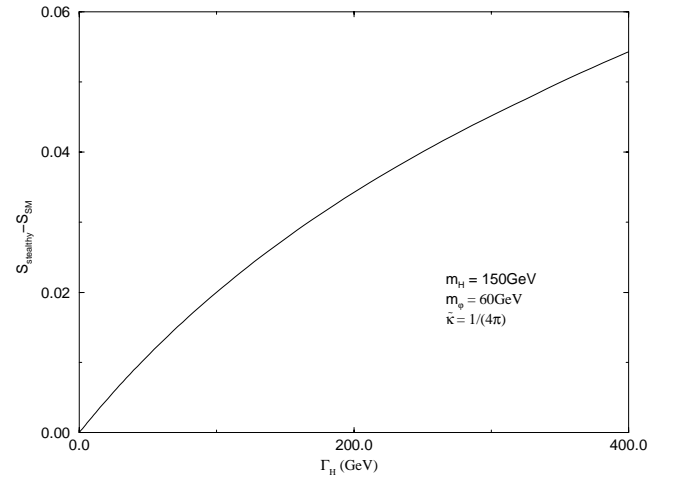


Fig. 9. Correction to the S parameter in the stealth model with self-interactions among the phions

mass case appears to be ruled out by the LEP precision data.

Finally Figs. 8–10 illustrate the κ dependence of the difference of the S and T parameters for the stealth and standard models. The conclusions here are the similar to the $\kappa = 0$ case.

Acknowledgements. This work was supported by the NATO grant CRG 970113, by a University of Michigan Rackham grant to promote international partnerships, by the US Department of Energy and by the European Union contract HPRN-CT-2000-00149.

Appendix

In this appendix we will discuss the question of the renormalization of the Higgs propagator spectral density in some more detail than in the main text.

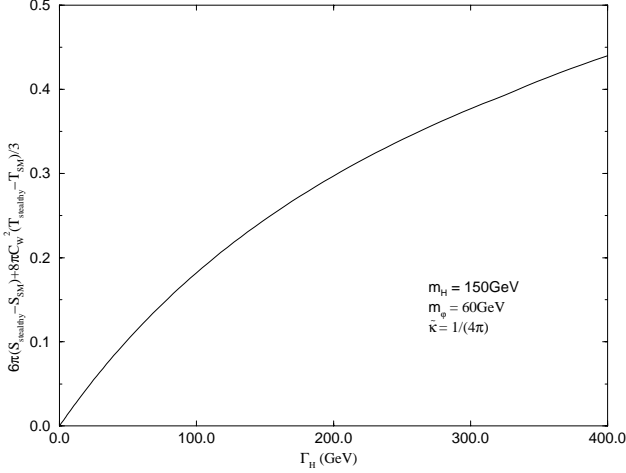


Fig. 10. Correction to a (large) Higgs mass independent quantity in the stealth model with self-interactions among the phions

It was argued in Sect. 3.4 that a necessary condition for the finiteness of the theory is

$$\int \sigma(s') ds' = 1. \quad (18)$$

Since the resummed propagator contains a tachyon pole which is an artifact of the approximation procedure, we choose to subtract this pole. The resulting spectral density $\sigma'(s')$ is however not properly normalized. Indeed, let us note that we may write for the inverse propagator near a zero at $k^2 = -m^2$:

$$D_H^{-1}(k^2) = (k^2 + m^2) \left(1 + \int \frac{1}{k^2 + \mu^2 - i\epsilon} \lambda(\mu^2) d\mu^2 \right). \quad (19)$$

One can relate the $\lambda(\mu^2)$ to $\sigma(\mu^2)$ by considering the imaginary part of the above:

$$\begin{aligned} \text{Im} D_H^{-1}(k^2) &= -\frac{\text{Im} D_H(k^2)}{|D_H(k^2)|^2} = \frac{-\pi \sigma(-k^2)}{|D_H(k^2)|^2} \\ &= \pi(k^2 + m^2) \lambda(-k^2), \end{aligned} \quad (20)$$

or

$$\lambda(\mu^2) = \frac{\sigma(\mu^2)}{(\mu^2 - m^2) |D_H(k^2)|^2}. \quad (21)$$

The contribution to λ from the two-body cuts can now be easily obtained from that of σ :

$$\lambda_2(\mu^2) = \frac{\Gamma(\mu^2)}{\mu^2 - m^2}. \quad (22)$$

In the above, for the case of massless phions with only three-point interactions, $\Gamma(\mu^2) = \Gamma$ introduced earlier, and for the case of massive phions,

$$\Gamma(\mu^2) = \Gamma \left(1 - \frac{4m_\phi^2}{\mu^2} \right)^{1/2}. \quad (23)$$

We thus get the following in the approximation of keeping only the two-body cuts:

$$\begin{aligned} D_H^{-1}(k^2) &= (k^2 + m^2) \\ &\times \left(1 + \int_c^\infty \frac{\Gamma(\mu^2)}{(k^2 + \mu^2 - i\epsilon)(\mu^2 - m^2)} d\mu^2 \right). \end{aligned} \quad (24)$$

For massless phions the lower cut c is 0 and for massive ones it is $4m_\phi^2$. The residue z of the propagator at a pole $k^2 = -m^2$ is given by ($k^2 = -s$)

$$z^{-1} = \left. \frac{-d}{ds} D_H^{-1}(s) \right|_{s=m^2}. \quad (25)$$

As an example, the residue at the tachyon pole $m_T^2 = -s_0 m_H^2$ is easily seen to be as follows for massless phions:

$$z^{-1} = 1 + \frac{\Gamma}{s_0 m_H^2}. \quad (26)$$

Now we are ready to determine the renormalization of σ' (call it $\bar{\sigma}$) such that $\int \bar{\sigma}(s') ds' = 1$. Noting that at a pole $s' = m^2$, $\sigma(s') = z \delta(s - m^2)$ we get, if such is pole is to be removed,

$$1 = \int ds' \sigma(s') = z + \int ds' \sigma'(s'). \quad (27)$$

From this we see that

$$\bar{\sigma} = \left(\frac{1}{1 - z} \right) \sigma'. \quad (28)$$

As discussed in Sect. 3.4 it gives the renormalization factor of $(\Delta + s_0)/\Delta$ for the tachyon in the massless phion case.

Such a procedure is quite general and may be used for any number of consistent subtractions. Thus if there are multiple unphysical poles that we wish to remove, then the corresponding renormalized spectral density may be written as

$$\bar{\sigma} = \left(\frac{1}{1 - \sum z_i} \right) \sigma', \quad (29)$$

where the z_i denote the z -factors at the positions of these unphysical poles.

When the complete model is treated, i.e., the four-point couplings are included and the phions are massive, the unphysical pole structure is much more complicated. The corresponding pole positions, spectral functions and the z_i functions may be obtained from the description of the model in Sect. 1. We will summarize the various cases below.

(1) $\tilde{\kappa} = 0, m_\phi = 0$. In this case as discussed earlier there is only one tachyon pole.

(2) $\tilde{\kappa} = 0, m_\phi \neq 0$. Here again there is only one pole. Define

$$\Gamma_2 = \frac{m_H^2}{c_H - 2}$$

and

$$c_H = r(m_H^2) \ln \frac{1 + r(m_H^2)}{1 - r(m_H^2)}.$$

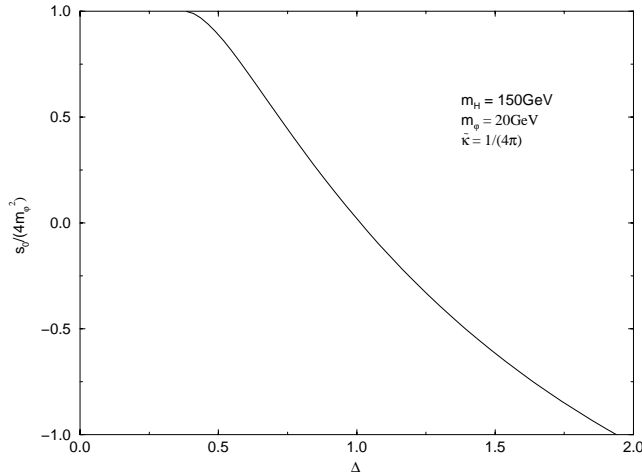


Fig. 11. Change of pole position due to variation of the parameters

Then when $\Gamma > \Gamma_2 > 0$, the pole is a tachyon, otherwise when $\Gamma_2 < 0$ the pole is physical as well as in the case when $\Gamma < \Gamma_2$ and $\Gamma_2 > 0$.

(3) $\tilde{\kappa} \neq 0, m_\phi = 0$. In this case there are always two tachyonic poles.

(4) $\tilde{\kappa} \neq 0, m_\phi \neq 0$. This is the most general case. Here, there are always two poles. One pole is always tachyonic and the other one behaves as in (2). Let us define \bar{s} as the solution to

$$1 + \tilde{\kappa}a(\bar{s}) = 0.$$

Then the tachyonic pole is always located to the left of $-\bar{s}$. The other pole can be tachyonic or physical, depending on the region of parameter space. This phenomenon, where the pole switches from unphysical to physical and vice versa has been noted earlier in [6]. In Fig. 11, we have depicted an example of how the pole positions change in this manner as the parameters of the theory are varied. Of course the subtraction procedure introduced earlier and the subsequent renormalization must be carried out only

for the unphysical poles. If s_i denote the positions of the unphysical poles, then the corresponding renormalization factors z_i are given by

$$z_i^{-1} = 1 + \frac{\Gamma}{[1 + \tilde{\kappa}\bar{a}(s_i)]^2} \left(\frac{1}{s_i} - \frac{2m_\phi^2}{s_i^2 \bar{r}(s_i)} \ln \frac{1 + \bar{r}(s_i)}{\bar{r}(s_i) - 1} \right), \quad (30)$$

where

$$\bar{r}(s) = \sqrt{1 + \frac{4m_\phi^2}{s}},$$

and \bar{a} is the same as a with the replacement $r \rightarrow \bar{r}$.

References

1. P. Igo-Kemenes, ICHEP2000, Osaka 2000
2. A. Gurtu, ICHEP2000, Osaka 2000
3. A. Hill, J.J. van der Bij, Phys. Rev. D **36**, 3463 (1987)
4. R. Casalbuoni, D. Dominici, R. Gatto, C. Giunti, Phys. Lett. B **178**, 235 (1986)
5. R.S. Chivukula, M. Golden, Phys. Lett. B **267**, 233 (1991)
6. R.S. Chivukula, M. Golden, D. Kominis, M.V. Ramana, Phys. Lett. B **293**, 400 (1992)
7. J.D. Bjorken, Int. J. Mod. Phys. A **7**, 4189 (1992)
8. R. Akhoury, B. Haeri, Phys. Rev. D **48**, 1252 (1993)
9. T. Binoth, J.J. van der Bij, Z. Phys. C **75**, 17 (1997)
10. N.V. Krasnikov, Mod. Phys. Lett. A **13**, 893 (1998)
11. J.F. Gunion, Phys. Rev. Lett. **82**, 1084 (1999)
12. M. Einhorn, Nucl. Phys. B **246**, 75 (1984)
13. M. Einhorn, H. Katsumata, Phys. Lett. B **181**, 115 (1986)
14. P. Cho, Phys. Lett. B **240**, 407 (1990)
15. K. Aoki, S. Peris, Z. Phys. C **61**, 303 (1994)
16. J.J. van der Bij, M.J.G. Veltman, Nucl. Phys. B **205** (1984)
17. J.J. van der Bij, Nucl. Phys. B **248**, 141 (1984)
18. J. Schwinger, Phys. Rev. **82**, 664 (1951)
19. S. Chadha, P. Olesen, Phys. Lett. B **72**, 87 (1977); P. Olesen, Phys. Lett. B **73**, 327 (1978)